EJSIT
European Journal of Science, Innovation and Technology
ISSN: 2786-4936
www.ejsit-journal.com
Volume 3 | Number 4 | 2023

Atmospheric Cyclone Driven Off Shelf and Off Continental Margin Oceanic Mass Flux Events in the Mid-Atlantic Bight U.S.A.

L. J. Pietrafesa[1,2], P. T. Gayes[1], S. Bao[1], T. Karl[1], L. Arencibia-Perez[1]
[1]Coastal Carolina University, Center for Marine Studies,
Conway South Carolina, United States
[2]North Carolina State University, Department of Marine, Earth & Atmospheric Sciences,
Raleigh, North Carolina, United States

ABSTRACT

The movement of sediment across the continental margins of the United States (U.S.) has been studied by numerous investigators over the past four decades. The classic, comprehensive review of the state of understanding was first provided by Smith (1977). Over that period, there have been several mid-latitude field programs studying the flux of momentum and materials across continental margins staged on both the east and west coasts of the United States. We will consider a data set that has been sitting idle for several decades but is intriguing as it couples atmospheric cyclone passages in the U.S. Eastern Atlantic Continental Margin, Middle-Atlantic Bight, to continental margin offshore fluxes of sediments; an overlooked and difficult to measure phenomena. Along the mid-latitude eastern seaboard of the U.S., there have been three large scale efforts to observe processes related to the flux of momentum and mass across the continental margin covering the region from Cape Cod, Massachusetts to Cape Hatteras, North Carolina. The first two studies were called the Shelf Edge Exchange Program, aka, SEEP I & II. SEEP I was staged between the New York Bight and southern Connecticut and is described by Walsh *et al.* (1988). SEEP II occurred offshore of the Delmarva Peninsula and is described by Biscaye *et al.* (1994). The Ocean Margins Program, aka the OMP, the third such effort, was staged between Chesapeake Bay, Virginia and Cape Hatteras, North Carolina and is described by Verity *et al.* (2002). All three field programs were sponsored by the U.S. Department of Energy. Traditionally there have been two schools of thought regarding the flux of materials on continental margins. One is the hypothesis that there is continual mass transport driven by costal oceanic currents and waves. The second purports that highly energetic events dominate the mass transport time series but offers scant observations to support that hypothesis. We investigate oceanic current and wave data, and cleverly designed sediment trap data, collected on the continental margin of the Middle Atlantic Bight and determine that the mechanisms associated with large accumulations of Lead 210 or 210_{Pb}, which is derived from the atmosphere, were delivered via an offshore directed flux of sediments. We show that lateral fluxes of sediments which occurred during the passages of high energy atmospheric cyclones were responsible for mechanically driving the across-continental fluxes of sediments.

Keywords: Sediment Transport, Extra-Tropical Cyclones, Tropical Cyclones, Mass Flux, Bottom Boundary Layer

INTRODUCTION

The movement and resuspension of sediment over the continental shelf of the U.S. eastern seaboard Mid-Atlantic Bight (MAB) has been studied by several investigators. A 1970's study by Butman *et al.* (1979) found that bottom sediment movement in the MAB often occurs over the outer shelf during large atmospheric wind events and are accompanied by a robust gravity wave field and energetic sub-inertial frequency bottom currents, particularly during winter. That study also found that sub-inertial frequency current speeds were significantly lower during summer than during winter, but internal waves were observed during

stratified summer conditions with bottom currents sufficiently large enough to suspend bottom sediments, but the movement of sediments did not seem to be very robust. Several studies (Anderson *et al.*, 1988; Biscaye *et al.*, 1988) discussed the mixing of sediment particles and the flux of the particles to the continental shelf and slope in the MAB over the SEEP-I experiment between 1983 and 1984 off of the Southern New England coast. A more detailed description of the SEEP-I study is presented by Walsh *et al.* (1988). The 1988-89 SEEP-II experiment attempted to focus on processes affecting sediment transport and resuspension in the more southerly Delmarva region of the MAB. It is of note that in the MAB, continental shelf waters are separated from offshore slope waters by a temperature-salinity Shelf/Slope Front (the SSF), as described by Houghton *et al.* (1994), and the transfer of mass directly across the front is, by definition, mechanically difficult. Physical phenomena are required to break the SSF down and allow for onshore to offshore transport across the SSF. Attempts were made during the SEEP-II experiment to test various alternative hypotheses related to various advective events, as explained by Houghton *et al*. (1994), such as the entrainment of shelf water, by passing warm core eddies via sinking across the SSF or via advection in the bottom boundary layer. But none proved to be operative in the various shipboard based and sampled data sets.

Oceanic continental margin sediment accumulations had been found (Butman *et al*., 1979) to be affected by resuspension events caused by severe weather conditions and near bottom and interior wave and current conditions in the MAB. Flow involving near bottom velocities greater than a critical value was found to lead to resuspension of fine particles, and this critical value was found to be about 17 cm/s by McCave (1972). A follow on study by Luyten (1977) calculated the root mean square (rms) of current velocities $\left(< u'^2 > + < v'^2 >\right)^{1/2}$ over different bottom depths on the MAB continental shelf and slope and found that mean near bottom current velocities are much weaker than the rms fluctuation and roughly once each month velocities greater than the critical velocity prevailed for several days in succession. Similar results were obtained over the Scotian shelf (Smith and Petrie, 1982), the Peruvian coast (Brink, 1982), and Georges Bank (Butman *et al.*, 1982), respectively. Numerical modeling experiments were conducted by Shaw and Csanady (1983) and determined that the near bottom flow in the MAB was affected more by a steep bottom slope than by the pressure gradients associated with steady oceanic currents representative of the MAB. Using SEEP-II near bottom current speed and surface wave height spectra data, Churchill *et al.* (1994) found that gravity waves and currents both contributed significantly to bottom stress generation and sediment resuspension over the continental shelf of the MAB out to a depth of 130 m. In addition, the authors suggested that high energy wind stress could induce shelf-wide sediment resuspension, though no effort was made to link actual atmospheric phenomena, such as atmospheric storms, to observed resuspension events. Again, the cases of the high energy currents and waves were not presented or even considered. However, such cases of high energy atmospheric and oceanic events are not unknown in U.S. continental margins, specifically in the MAB.

High energy continental margin oceanic events may be related to the passages of highly energetic atmospheric storms, such as wintertime extra-tropical cyclones (ETC's) also known variously as "Atlantic Lows", or "Hatteras Lows", "Cyclogenetic Bombs" or "Nor'easters" and summertime and fall tropical cyclones (TCs). Several studies (Sanders and Gyakum, 1980; Roebber, 1984; Cione *et al.*, 1993; Cione, 1996) found that the ETC storms occur principally during the months of October through April and are often formed via an atmospheric - oceanic coupled process called cyclogenesis and can occur when incoming ETCs are further intensified in the coastal region extending from Georgia (GA) to New Jersey (NJ), centered about Cape Hatteras North Carolina (NC). These events occur on the order of several tens of times per year

(Cione *et al.*, 1993). Annually, from June to November, several North Atlantic Ocean Basin tropical cyclones (TCs) venture into the MAB area, often maintaining hurricane strength. The study reported on by Cione (1996) showed that over the 1981-1993 period, the bulk of the 718 ETC storms observed in the western North Atlantic passed through the 10˚ x 10˚ block 32.5˚-42.5˚ N x 67.5˚ to 77.5˚ W. Further the studies by Cione *et al.* (1993) and Cione (1996) showed that 391 of the total number of ETC's were actually spawned in the smaller region west of 70˚ and south of 37.5˚ N, focused offshore of Cape Hatteras. The mean ETC track was found to be along the South-Southwest (SSW) to North-Northeast (NNE) axis, passing 100 km to the east of Cape Hatteras. As ETC storms move west to east and south to north, and as a function of storm track and storm size, winds over the U.S. East coast shelf/slope are generally north-northeast to south-southwest (i.e., nominally "northeasterly"). So, as the storms move to higher latitude, the wind field is directed down-shelf with an ever-increasing fetch until the storm clears New England. This may have important implications for the transport and dispersal of mass along, across and off the MAB.

The study reported on herein, calculates the bottom boundary layer offshore transport and the bottom current velocity fluctuation associated with alongshore barotropic - geostrophic interior flows and resulting bottom currents. It also reports on a highly suggestive correlation between the passage of ETC atmospheric low-pressure systems, which were observed to be present in the large region bounded by 30˚ to 45˚ N latitude and 60˚ to 80˚ W longitude and encompassing the SEEP II study area. This study employs SEEP II current meter data to qualitatively explain fluctuations in the sediment trap data presented by Biscaye and Anderson (1994). However, unlike the results reported on by Cione (1996), this study is not concerned with the details of the geochemistry of what was collected. Rather the focus herein is only on, how much, was collected by each of the set of sediment trap cups which opened and closed at a set time, in sequence, across the entire SEEP II array. This configuration and cross-array temporal opening and closing were very cleverly designed as described below. The results of our study strongly suggest a robust storm response to sediment motion in the MAB and speak to storm related mass wasting high energy events being responsible for significant offshore fluxes of sediments, rather than continual low energy fluxes, which is an alternative hypothesis described by Smith (1977).

THE SHELF EDGE EXCHANGE PROCESSES (SEEP-II) EXPERIMENT

The Shelf Edge Exchange Processes (SEEP-II) experiment was conducted in the shelf and slope regions of the Delmarva Peninsula and Virginia from February 1988 to May 1989, and was the second and final experiment in the U.S. Department of Energy-sponsored SEEP program. A complete program description can be found in the study by Biscaye *et al.* (1994). The SEEP-II experiment consisted of an array of 10 mooring sites (north line moorings 1-7 and south line moorings 8-10, as shown in Figures 1 and 2. The SEEP-II current meter mooring array was designed so that cross-continental margin mass transport could be addressed. The purpose of the program was to examine the possible cross-shelf transport of carbon, biological-physical interactions and frontal dynamics. The two cross shelf transacts were located perpendicular to the alongshore mean direction of the isobaths and separated by about 100 km. The south line triplet of moorings was located at the same depth as the three most seaward moorings on the north line. The north line location was selected to be several deformation radii away from large topographic irregularities such as submarine canyon heads along the shelf break, as indicated in Figure 1. The locations and the types of current meter are given in Figure 2 and are described by Verity *et al.* (2002). The current meter data at moorings 2, 3, 4, were obtained using upward looking bottom mounted RDI Acoustic Doppler Current Profilers (ADCPs), and the other current measurements were obtained using Aanderaa Recording Current Meters (RCMs) and Vector Measuring Current Meters (VMCMs). The interior

geostrophic current field measured at mid-depth at moorings 6 and 9 will be used to discuss the sediment accumulation data used in boundary bottom layer transport calculations. A 40-hour low pass filter (Biscaye and Anderson, 1994) was applied to all current time series. The oceanic tidal signal and other high frequency fluctuations with periods shorter than one day were filtered out. The time series was further subsampled into 6-hour data. The average alongshore current velocities at all of the moorings for all of the seasons were found to be an order of magnitude larger than those of offshore components so the sub-inertial frequency flow vectors were aligned principally along the isobaths (parabathic flow). In Figure 3, the total masses of the time weighted means of the sediments that accumulated in the sediment traps during SEEP II is presented. As can be seen, the highest mass flux accumulations were in the sediment traps at the bases of Moorings 5 and 9 where the totals were 3,358 and 4,467 mg/m^2/day, respectively. Moreover, the bottom traps at Mooring #5 were 1297, #7 was 1758, #8 was 2869, #10 was 1522. As explained below, according to Biscaye and Anderson (1994), these sediment accumulations also contained the highest amounts of 210_{Pb}. However, 210_{Pb}, is derived from the atmosphere, so the question arises, how were the sediments delivered to the sediment traps located at the bases of the moorings. This is the source of the quandary and one of the foci of this study.

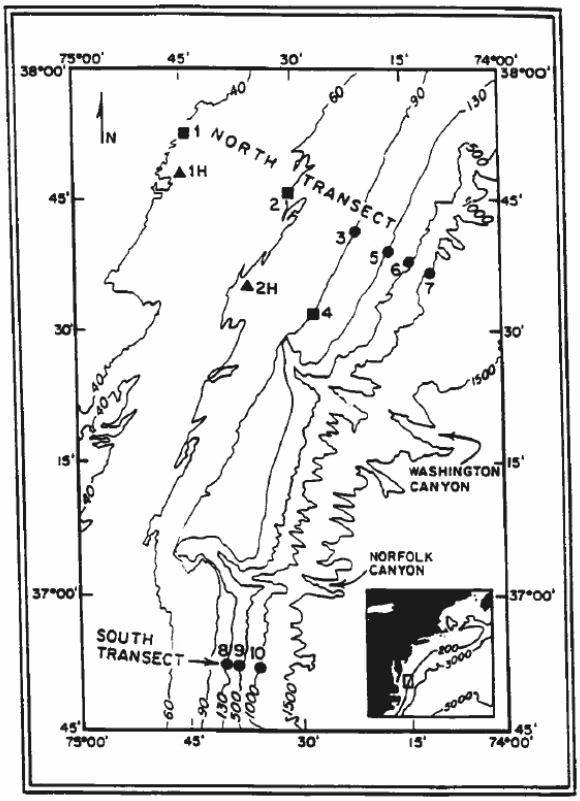

Figure 1. The SEEP II Mooring Array in horizontal perspective

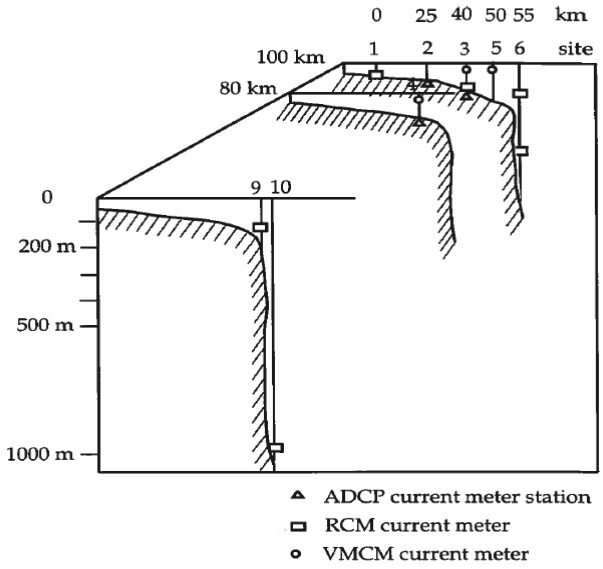

Figure 2. The SEEP II Mooring Array in vertical perspective

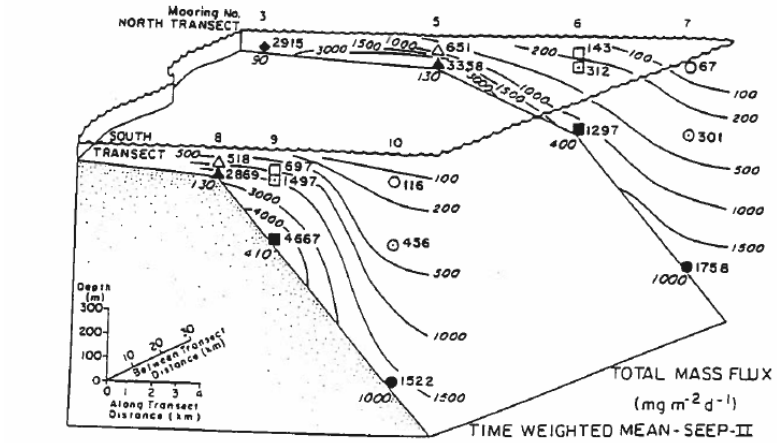

Figure 3. SEEP II Moorings and Total SEEP II time-weighted sediment deposits. The Sediment Traps are located on the Current Meter Moorings shown in Figure 2.

SEEP II Sediment Trap Data

During the SEEP-II experiment, from February 1988 to May 1989, 17 sediment traps were deployed at seven locations (Figure 3) and recovered three times as reported on by Biscaye and Anderson (1994). There were two 3-4 week intervals between the three deployment periods. The sediment records show three segments: February-May 1988; June-October 1988; and November-May 1989. As detailed by Biscaye and Anderson (1994), in each sediment trap, there were 10 cylindrical sampling tubes in a carousel. An electronic device controlled the rotation of the sampling carousel. The sampling interval was preset for each of the 10 sample tubes. The tube started collecting when it was rotated to the open (11th) carousel position, and all sample tubes were sealed off except when they are rotated to the open position. For each sediment segment, there are 10 data points. So, the total for the three segments are 30 data points. Since the study periods were of different lengths, based on ship availability, and recovery periods, the actual length of carousel sample tube openings varied between measurement periods, but was constant across the mooring array within any deployment

period. Again, we consider this to have been an ingenious design. In this study, we examine sediment accumulations as a function of possible sediment transport and resuspension. To do so concisely, we will employ the sediment mass flux data reported by Biscaye and Anderson (1994) from mooring 6 on the north line and from mooring 9 on the south line. Both of the moorings are located on the 400 m isobaths, with the traps set at the same 390 meters. These sites are utilized because they are representative of all of the others and the current meter and trap records are complete.

The vertical flux of the particles during the total of 30 sampling intervals over the SEEP-II period between February 1988 and May 1989, using 210_{Pb} as a tracer of particles and fluxes to determine the source of sediments was reported on in the study by Biscaye and Anderson (1994). It reported that fluxes of 210_{Pb} to the upper slope sediments of MAB varied spatially by as much as a factor of two. A representative average flux of 210_{Pb} is about 3 (disintegrations per minute per cm^2 per year (or dpm cm^{-2} y^{-1}) to the bottom on the upper slope, but the atmospheric supply to the same region is less than one third of this number. They found that the flux of 210_{Pb} to the upper slope sediments is much larger than its local rate supply from the atmosphere, that the flux of 210_{Pb} to the upper slope is much larger than the downward flux of 210_{Pb} measured by the shallower sediment trap and that the 210_{Pb} flux in the SEEP-II region is a factor of two larger than that of SEEP I region (farther north). This lead (Biscaye and Anderson, 1994) to the conclusion that most of the 210_{Pb} deposited on the upper slope is supplied by some form of lateral or offshore, transport. However, the physical, dynamical mechanisms were not identified by Biscaye and Anderson (1994). Moreover, additional evidence for the importance of lateral/offshore transport for sediment accumulations in the MAB were not identified as the authors claimed that the biogenic components of total mass flux should not increase with depth, because they are principally produced in near surface waters. However, the SEEP II data showed that the flux of biogenic and other particulates increase with depth in the water column despite the fact that their concentrations decrease downward through the water column. So, quandaries were created and existed to the present. But below, we reveal the relationships between storms and sediment accumulations.

Meteorological Data and Oceanic Current Meter Data during SEEP II

In Figure 1 and Figure 2 the SEEP II horizontal and vertical, respectively, bottom mounted current meter moorings, sediment trap mooring locations and meteorological buoy network are displayed. Wind data measured from the Chesapeake Light Station (CHL) for the SEEP II winter and spring periods are presented in Figure 6, by way of example, with cyclone dates indicated. The winds are decomposed into “along coast”, that is, North-Northeast (NNE) to South-Southwest (SSW), with NNE positive (+) up and SSW (-) down (bottom panel) and onshore-offshore winds or those perpendicular to the coast as East – Southeast (ESE) with positive (+) values (ESE) and negative (-) values to the West-Northwest (WNW) (middle panel). From the wind stick plots, with NNE up, etcetera, (top panel), we can see the time history of winds as the ETCs and TCs passed through the region during this period of SEEP II. As described above, a 40-hour low pass filter described by Pietrafesa *et al.* (1976) was applied to all wind and oceanic current time series, so that the oceanic tidal signal and the inertial signal and other high frequency fluctuations with periods shorter than 40 hours are suppressed. The time series was then subsampled at 6 hours. In addition to the wind field measured at the fixed NOAA coastal buoy and lighthouse stations, we employed surface weather maps published by NOAA (not shown) to display the atmospheric surface pressure during the cyclone events to determine geostrophic wind directions. During the 30 sediment measurement intervals over the February 88 - May 89 period, there were 26 ETCs and 3 TCs which passed in the general vicinity of the SEEP II mooring array. An example of the individual ETC tracks are plotted by for the month of March 1988 and of the individual TC tracks for July and August 1989 in

Figures 4 a, b. We only show the March 1989 period of 7 ETC passages as they are representative of the other 21.

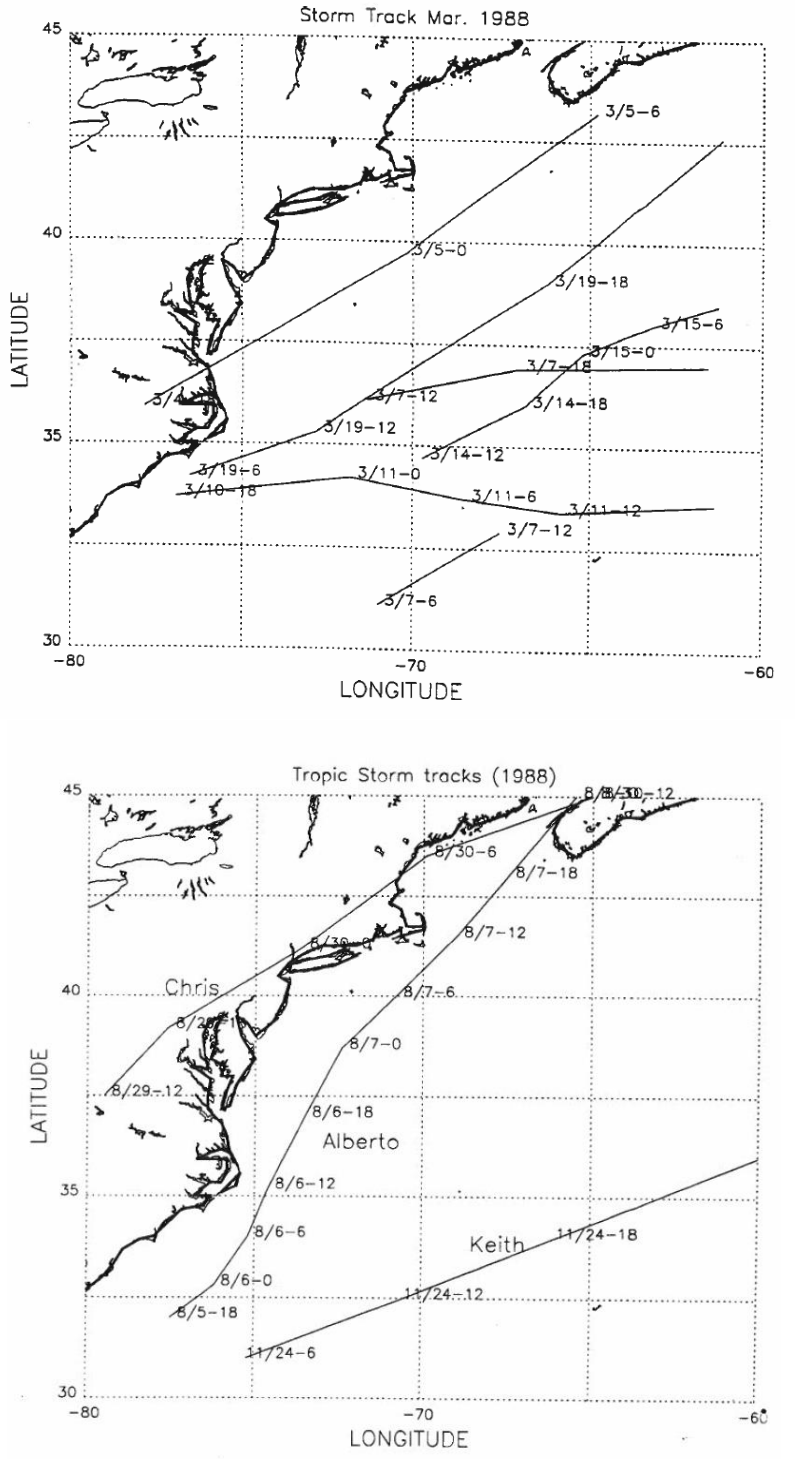

Figure 4. Atmospheric Cyclone passages. Left Panel: 7 ETC events during March 1989. Right Panel: 3 TC events during the Summer/Fall 1988.

At all fixed horizontal points on the continental margin, including the SEEP-II mooring sites, the winds associated with passages of either ETCs or TCs will change direction as a function of time as the storms pass by. As a function of storm size, path and shape, the time histories of winds can be very different at different locations over the MAB. For example, if the storm axis was along the continental margin from southwest to northeast, but the storm eye

was to the east and offshore of the mooring array then the time series of winds would be westward, southwestward, southward and southeastward as the storm progressed. If this type of storm were sufficiently large, then the entire MAB could be affected by strong southward winds and the mooring array instruments could reflect similar results of the transport for both north and south lines. Also though, a cyclonic storm could pass between the north and south lines and thus the time series of winds and perhaps associated flow fields would be quite different. To be clear, wind vectors rotated clockwise or counter-clockwise during the passage of a cyclone event, as a function of which side of the axis of flow around the cyclone center or Eye, the CHL wind station was located. Clearly, many scenarios possible are the u, v response to the cyclone passages and subsequent forcing depends on whether the storm tracks are to the left, in the middle or to the right of the individual moorings. For the record, if a monitoring station is on the left side (right side) of a passing cyclone, then the wind vectors will rotate counter-clockwise (clockwise) as a function of time. Therefore, cyclones do not manifest themselves via counter-clockwise wind vector rotations. Rather it depends on which side of the passing cyclone that the wind vector measurements are taken. The wind statistics are summarized in Table 1. Given their temporally average tracks, which is to the right of the mooring array, the ETCs produce winds which are favorable for driving down shelf currents, parabathic flows, and gravity wave propagation, i.e., from north-northeast to south-southwest in the MAB, as shown in the Figure 5 lower panel ("Alongshore").

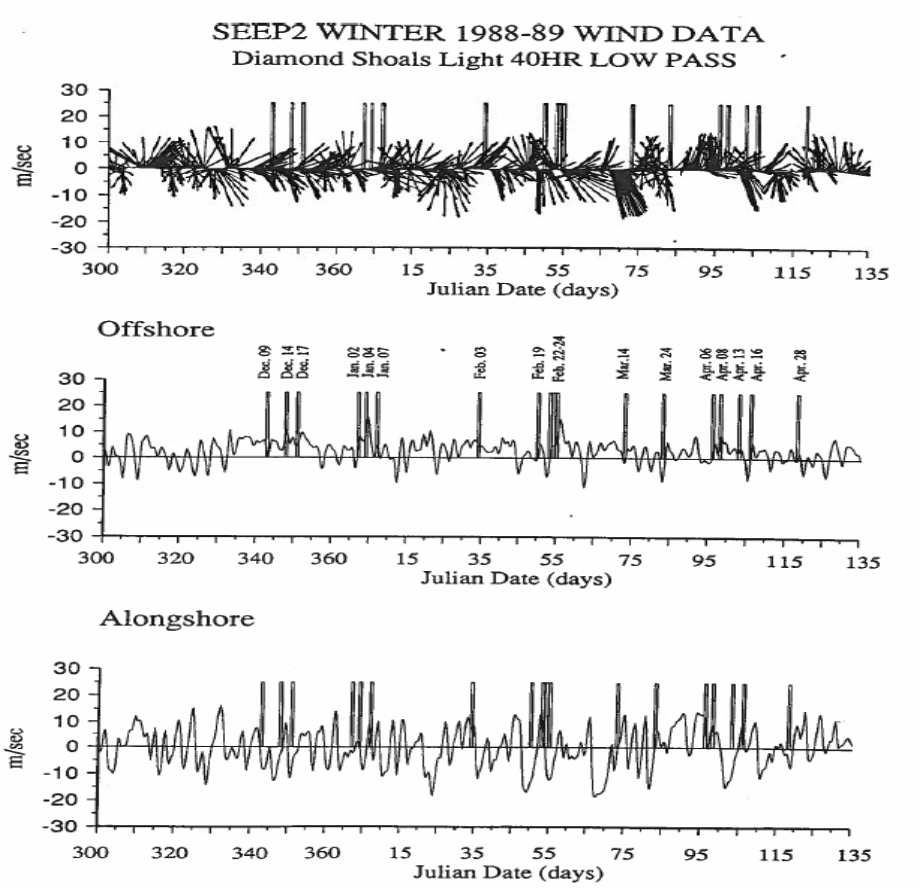

Figure 5. Wind data from Diamond Shoals from Julian Days 300 – 366 in 1988 and 0 – 135 n 1989 (27 November 1988 – 15 May 1989). The data is aligned 30º east of north (upward in the plot and positive alongshore), 30º west of south (downward in the plot and negative alongshore), and east-southeast (positive offshore) and west-northwest (negative onshore). The dates of 16 ETC passages are indicated by the vertical lines and dates. The vertical axes are in meters/second (m/sec).

Atmospheric cyclone statistics defining the storm date, storm central pressure drops in the study area and duration of the storms passing through the SEEP-II region are summarized in Table 1. We can see that there were 26 ETCs and 2 TCs which passed through the MAB, in the vicinity of SEEP-II moorings, during the period February 1988 - May 1989. NOAA atmospheric pressure maps (not shown) allow us to determine the size of each individual storm relative to its track given previously in the sequence of Figures 4 a, b. Figure 4a only shows the storm tracks of 6 of the ETCs during March 1988, by way of example, of the total number of 26 ETCs. The cyclone track and surface analysis showed that 24 out of 26 extratropical cyclone events produced winds which appear to have been favorable for the alongshore and offshore transport and/or local resuspension of sediments which then accumulated in the sediment traps at sites 6 and 9. In 22 of the 26 cases of ETC passages, traps filled up at both sites. Alternatively, there were 2 ETC events which did not correlate with increases in sediment accumulations in the traps but rather with decreases in the accumulations. These two ETCs occurred on 10 May 1988 and 03 February 1989. From the cyclone track analysis (not shown) it is clear that the May 18, 1988, cyclone followed a track that was to the southeast, which is an unusual direction for a MAB ETC. The atmospheric pressure surface map analysis (not shown) indicates that the cyclone size was small, its diameter being only one fourth of the size of the average winter cyclone and it was well to the south of the SEEP-II mooring array. This particular cyclone produced no favorable wind direction for down shelf and offshore transport in the SEEP-II experiment region (Figure 1). The February 3, 1989, cyclone passed through the SEEP-II experiment area, but the storm was extremely weak. The size of this cyclone was also very small. In both cases, the one-day normalized storm central pressure deepening rate was very small, apparently rendering the storms ineffectual, in creating a robust oceanic response.

Table 1. ETC and TC Tracks and Atmospheric Characteristics

	Storm Date	Julian Day	Pressure Drop dp (mb)	Normalized dp/dt (mb/day)	Duration (hours)	Deposition rate (North/South)	Storm Radius (KM)	Track Position (North/South)	Favorable Wind (North/South)
1	Feb. 27, 1988	58	0	0	18	up/up	550	Right/Right	Yes/Yes
2	Mar. 4, 1998	63	-4	-16	6	up/up	N/A	Right/Right	Yes/Yes
3	Mar. 7, 1988	66	-9	-108	2	up/up	N/A	Right/Right	Yes/Yes
4	Mar. 19, 1988	78	-3	-9	8	down/up	170	Right/Right	Yes/Yes
5	Apr. 7, 1988	97	0	0	24	stays up/stays up	490	Right/Right	Yes/Yes
6	Apr. 18, 1988	108	-1	-0.9	28	stays up/stays up	N/A	Right/Right	Yes/Yes
7	May 6, 1988	126	-6	-4.5	32	up/down	750	Center/Center	Eye/Eye
8	May 18, 1988	138	-2	-2	24	down/down	120	Bottom/Bottom	No/No
9	Aug. 7, 1988	219	-4	-5.3	18	up/down	100	Right/Right	Yes/Yes
10	Aug. 29, 1988	241	-1	-2	12	down/up	N/A	Left/Left	No/No
11	Dec. 9, 1988	343	-9	-72	3	up/up	N/A	Right/Right	Yes/Yes
12	Dec. 14, 1988	348	-8	-64	3	up/up	720	Right/Right	Yes/Yes
13	Dec. 17, 1988	351	-6	-48	3	up/up	N/A	Right/Right	Yes/Yes
14	Jan. 2, 1989	2	-7	-9.3	18	up/up	600	Right/Right	Yes/Yes
15	Jan. 4, 1989	4	0	0	3	up/up	640	Right/Right	Yes/Yes
16	Jan. 7, 1989	7	-6	-12	12	up/up	500	Top/Top	Yes/Yes
17	Feb. 3, 1989	34	-1	-1.1	21	down/down	70	Center/Center	No/No
18	Feb. 19, 1989	50	-5	-6.7	18	up/up	520	Right/Right	Yes/Yes
19	Feb. 22., 1989	53	-1	-1.3	18	up/up	210	Center/Center	Yes/Yes
20	Feb. 23, 1989	54	0	0	3	up/up	460	Right/Right	Yes/Yes
21	Feb. 24, 1989	55	-6	12	12	up/up	730	Right/Right	Yes/Yes
22	Mar. 14, 1989	73	-2	-2.6	18	up/up	350	Right/Right	Yes/Yes
23	Mar. 24, 1989	83	-5	-7.5	16	stays up/stays up	520	Right/Right	Yes/Yes
24	Apr. 6, 1989	96	-6	-8	18	up/up	N/A	Right/Right	Yes/Yes
25	Apr. 8, 1989	98	-7	-14	12	up/up	380	Right/Right	Yes/Yes
26	Apr. 13, 1989	103	-3	-12	6	up/up	N/A	Right/Right	Yes/Yes
27	Apr. 16, 1989	106	0	0	6	up/up	N/A	Right/Right	N/A
28	Apr. 28, 1989	118	0	0	15	up/up	N/A	Right/Right	Yes/Yes

What is common amongst all the well correlated cases of ETC passage is down shelf, alongshore winds (Figure 5, by way of example). In Figures 6a, 6b, the low-passed oceanic currents at the base of current meter moorings 6 and 9, are shown. Figures 6, left panel, and right panel, are for the late winter 1988 and early spring of 1989, by way of example. Common are offshore near bottom flows during the periods of ETC passages. What is demonstrated is that as an ETC transects the MAB, winds are predominantly down shelf and the near bottom currents are down shelf, in-kind, and offshore in the Bottom Boundary Layer (the BBL). Mechanically driven near surface currents are down shelf and coastward, in the direction of the wind and to the right of the wind, in a surface time dependent Ekman Layer respectively (not shown but explained by Janowitz and Pietrafesa (1996). From Figure 6, we can see the bottom alongshore currents at both the north and south lines were to the south-southwest (-V) and an order of magnitude larger during the storm event periods than those during the non-storm event periods. The same is true of the offshore velocity (+ U), suggesting a net offshore transport and its magnitude during the storm periods compared to the non-storm periods. The U and V current components appear to be in sync with when V is negative, U is positive. The Root Mean Square (RMS) bottom velocity and bottom stress computed using a quadratic drag law and were computed to show sediment resuspension events during the SEEP II experiment, as discussed below.

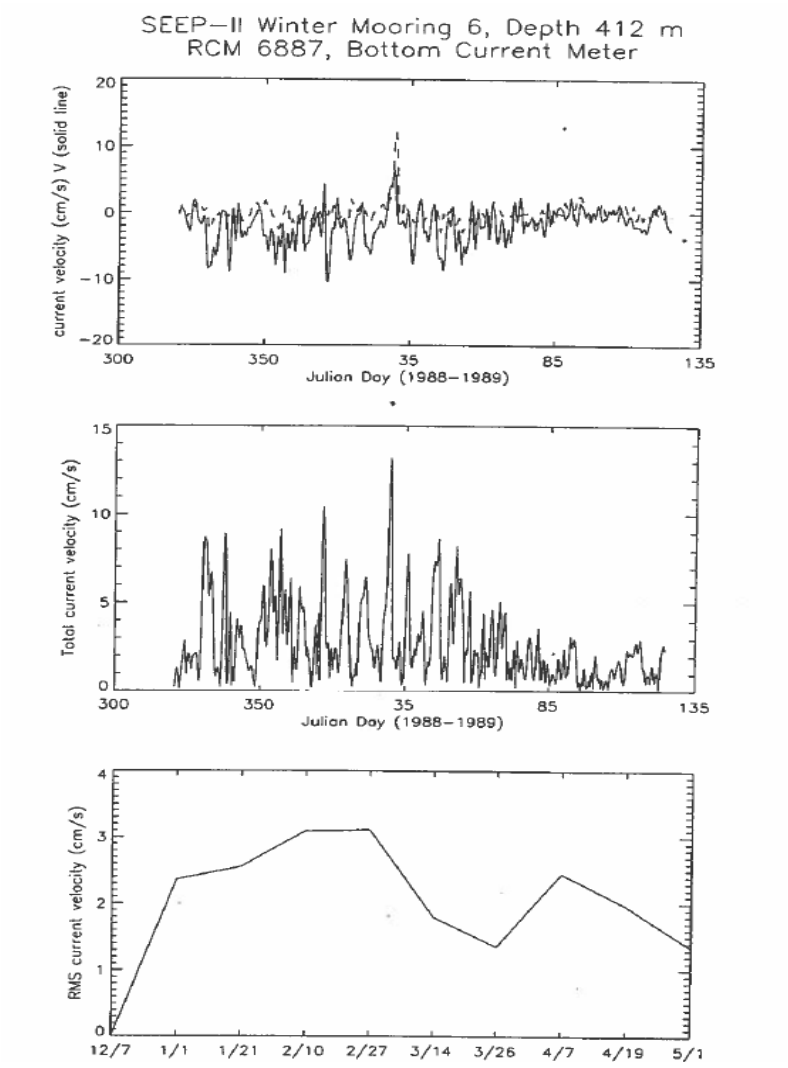

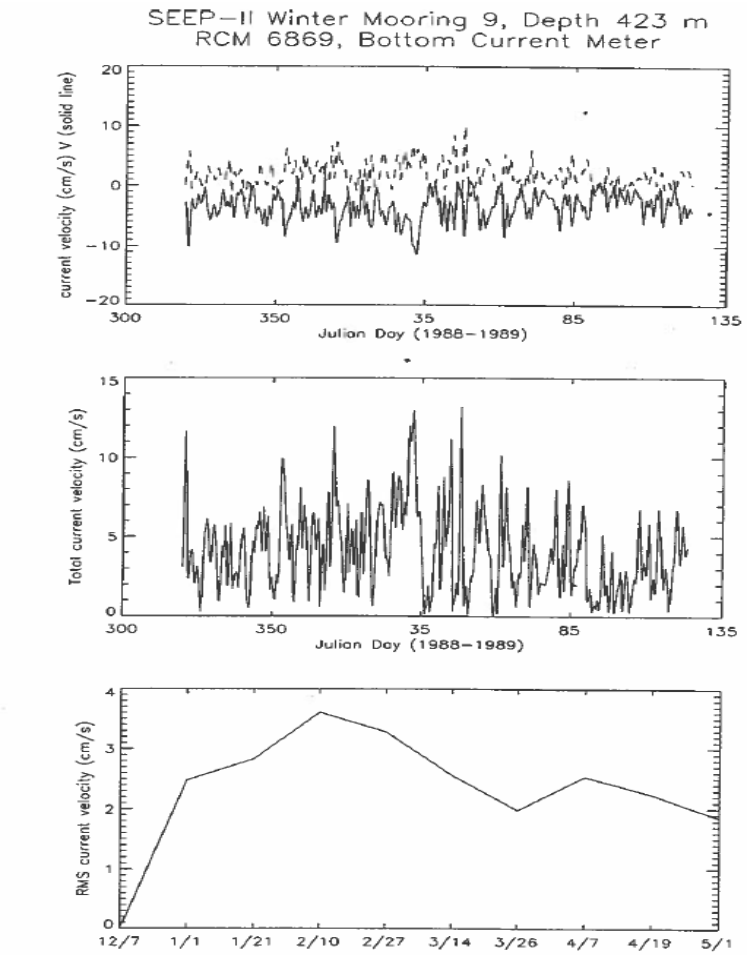

Figure 6. Current meter data from 2 meters above the bottom at Moorings 6 and 9. The currents are plotted as parabathic (solid lines in the upper panel) and diabathic (dashed lines in the upper panel). Total current speeds are in the middle panels. RMS velocities are in the lower panels. See the text for details.

We can see that the bottom RMS velocities at moorings 6 and 9 were generally small during the SEEP II experiment and the local resuspension event associated with the bottom current fluctuation is not a significant factor for sediment accumulation for most of the time on the upper slope of MAB over the SEEP II experiment. But during the two extreme events, the bottom RMS velocity reached its maximum and its magnitude was large enough to generate local resuspension, and thus possibly enhance the sediment accumulation rate.

We can compute the bottom stress using the quadratic law to evaluate the bottom forcing,

$$\tau = \frac{1}{2} \rho C_D U^2 \quad (1)$$

where τ is the current bottom stress, ρ is the density of water, U is the total current velocity, $(< u^2 > + < v^2 >)^{1/2}$, measured at the fixed depth of 10 m above the bottom, and C_D is a drag coefficient determined from bottom roughness and determined ia field measurements in the MAB by Janowitz and Pietrafesa (1996) to have a value between 0.0058 and 0.0094. Similar to the RMS velocity plot, the bottom stress can be estimated and is typically very small (less than 0.8 dy cm^{-2}) over the entire SEEP II experiment at the 400 m depth. There were few occasions when the bottom stress exceeded 1 dy cm^{-2}. The large bottom stress events happened around Julian 95, 1988 and 35, 1989, which corresponding to the two extreme periods mentioned previously.

There were two extreme periods when the sediment accumulation rate displayed very large peaks; during April 1988 and February 1989. From Figure 7 we see that during the April 1988 event, the averaged alongshore current reached its maximum (-V maximum) on both north and south lines. At mooring 6, the interior averaged current between 4/9 and 4/19 was over 20 cm/s, while at mooring 9, its value was about 8 cm/s. The strong alongshore interior current was favorable for bottom offshore Ekman transport. In addition, the offshore velocity (+U) also reached its maximum at both mooring 6 and 9. Oceanic temperature sensors at the different SEEP-II moorings (Figure 2) were analyzed by Houghton *et al.* (1994), and that study found that offshore water transport increased in the upper water column during the April 1988 event. Our calculation showed that the interior current also had an offshore current component, although its magnitude was about 2 cm/s and smaller compared to that of the alongshore current. Moreover, these current meter data will for the spring of 1988 will be compared below to the Sediment Trap data. The current meter time series at the bottom of Moorings 6 and 9 strongly suggest the setup and existence of an Ekman BBL, over all seasons. Herein we invoke BBL theory to calculate the offshore transport at each of locations 6 and 9.

Ekman BBL theory is presented by Pedlosky (1979). Here, the theory is used over the sloping bottom of the SEEP region to theoretically proscribe the amount and direction of mass transport associated with the interior mean flow. The point is that on the outer shelf and upper mid slope of the MAB, the bottom may be sufficiently steep to enhance across-slope/shelf diabathic transport. The Ekman layer thickness over a flat bottom is given by Lyne *et al.* (1990) as

$$\delta_E = \left(\frac{A_v}{f/2} \right)^{1/2} \tag{2}$$

where A_V is the vertical turbulent viscosity coefficient and f is Coriolis parameter. The bottom boundary layer presumably can act as a channel for offshore sediment transport. However, the theory must be adjusted to determine the Ekman layer thickness, for flow over a bottom of constant slope alpha with

$$Z_* = X_* \tan \alpha \tag{3}$$

and in dimensionless form is written as

$$z = x \frac{L}{D} \tan \alpha = x \tan \theta \tag{4}$$

Following Lyne *et al.* (1990), we can write the boundary thickness perpendicular to the slope as (5)

$$\ell^* = \delta_E (\cos \alpha)^{1/2} \left(1 + \frac{E_H L^2}{E_v D^2} \tan^2 \alpha \right)^{1/2}$$

$$= D \, x \left(2 \frac{A_v}{f D^2} \right)^{1/2} x (\cos \alpha)^{1/2} \left(1 + \frac{2 \frac{A_H}{f L^2}}{2 \frac{A_v}{f D^2}} \, x \, \frac{L^2}{D^2} \tan^2 \alpha \right)^{1/2} \tag{5}$$

$$\ell^* = \left(\frac{2 A_v}{f} \right)^{1/2} x (\cos \alpha)^{1/2} \left(1 + \frac{A_H}{A_v} \tan^2 \alpha \right)^{1/2}$$

where A_V and A_H are vertical and horizontal eddy viscosity coefficients, taken here as 10^2 and 10^5, respectively (Lyne *et al.*, 1990) and f is ~ 10^{-4}.

Here we see that over a sloping bottom we have a bottom frictional layer of thickness *l** which is a function of both vertical and horizontal eddy mixing which would erode the base of the MAB Shelf Slope Front (Houghton *et al.*, 1994), thereby allowing shelf water masses to

slide along the bottom underneath the SSF which presumably reestablishes itself into the bottom once the ETC induced event subsides. From equation (4), we can see the Ekman layer thickness is of the same order $\left[O\left(E_v^{1/2}\right)\right]$ as that for the flat bottom case, but is a more complex function of the bottom slope and the ratio of E_H to E_V. The Ekman layer depth is about 14 m for a flat bottom or 0^o slope and increases as the slope steepens. On the MAB shelf the slope varies as shown in Figure 3, approximately from 10^{-3} at the 100 m isobaths to 10^{-2} out at the 400 m isobaths. This result suggests that the Ekman layer depth is greater on the continental slope than that on the continental shelf. Therefore the offshore water transport channel is likely thicker and can be written as:

$$T = \frac{l^*}{2\cos\theta}\frac{\partial p}{\partial y} - \frac{l^*}{2\cos\theta}\frac{\partial p}{\partial x}\left(1-\delta^2\tan^2\theta\right)^{-1/2}$$
$$= \frac{l^*\left(1+\tan^2\alpha/\delta^2\right)^{1/2}}{2}\frac{\partial p}{\partial y} - \frac{l^*\left(1+\tan^2\alpha/\delta^2\right)^{1/2}}{2}\frac{\partial p}{\partial x}\left(1-\tan^2\alpha\right)^{-1/2} \quad (6)$$

For the MAB region, the current field flows predominantly along isobaths, the offshore velocity is small compared to the alongshore velocity. From Pedlosky (1979), we can see that the velocity field over the tilting bottom is similar to that over the flat bottom, and as the bottom is approached, the velocity vector turns to the left of the geostrophic flow within the Ekman layer. If $V < 0$ (flow to the southwest in the SEEP-II region) then $T > 0$, indicating positive offshore transport, else if $V > 0$ then $T < 0$, indicating onshore transport. Therefore, the total bottom transport is to the left of the geostrophic flow, and its magnitude is a function of the tilting slope and the geostrophic current velocity. In addition, the offshore bottom transport increases as the southwest alongshore flow (-V) increases.

Using the above BBL Transport Theory and Equation (6), we construct a BBL Transport time series for the spring 1989 time series as shown for the current meter at the bottom of Mooring 9. The plot for Mooring 6 is nearly identical to Mooring 9, so is not shown. There were eight ETC events during the SEEP-II spring 1988 deployment. From Figure 7 we can see that during six of eight ETC events, the transport reached its peak and the maximum transport occurred between Julian Days 97 and 108, corresponding to April 1988 when there were two ETC events and one of these was one of the two extremely intense ETC events which occurred during the entire SEEP-II experiment. In general, as suggested in Figure 6, the bottom current is typically weak with a mean velocity about 5 cm/s during the spring experiment and between 2 and 3 cm/s during the winter periods at both moorings 6 and 9. The mean current velocity for the winter period at these sites were between 2 and 3 cm/s. Again, the RMS velocity and time averaged RMS velocity at moorings 6 and 9 are shown in Figure 6. For the spring deployment, at mooring 6, we can see the time series of RMS velocity showed a big change over the entire period, with the maximum of about 10 cm/s in April 1988. The critical value to generate the local resuspension is of order 0 (10 cm/s) according to McCave (1972). Therefore, using 40 h low pass filtered data, currents with and RMS velocity of 10 cm/s would be large enough to exceed the critical value. Comparing these RMS velocity time series (Figure 6) with the BBL transport plot (Figure 7), we can see that both the RMS velocity and BBL transport reached their maxims in early April 1988. Both the increased BBL transport associated with the strong alongshore interior current and the local resuspension associated with the high RMS bottom currents would the account for the April 1988 event described by Biscaye and Anderson (1994). For the winter deployment, the time averaged RMS velocities at both moorings 6 and 9 were small and in the order of 2 to 3 cm/s. Although the time series of RMS velocity showed several peaks, the RMS velocity was lower than 10 cm/s. However, there is one exception, when the RMS velocity at mooring 6 reached its maximum around Julian day 35 1989, which could have

generated local resuspension during this period. This happened at the same time that the February ETC event occurred. The RMS velocity at mooring 9 on the south line never exceeded the 10 cm/s threshold and so flow conditions there were not favorable for suspension events.

Figure 8 is the documented Accumulation of Sediments in the Traps located at the Bases of Moorings 6 and 9 during the spring 1988 and the combined winter 1988 & spring 1989. For the spring 1988 deployment, we can compared BBL transport to the sediment accumulation rate plot in Figure 8. As shown the two sediment accumulation rates peaked occurred when the BBL transport also reached its peaks. The plot extends from Julian Day 45 (February 14) to Julian Day 159 (June 07). It is of note that the sediment accumulation rate was a minimum between March 31 and April 9, 1988, and between May 29 and June 6, 1988. The transport for the same period is less than zero which indicated that the flow had no southwest component during these two periods and thus no offshore BBL transport in an Ekman BBL. In Table 1, according the National Weather Service, there were 8 ETC events of note, centered about February 14 and 28, March 04 and 19, April 07 and 18 and May 06 and 18. The matching Julian Days (JDs), in Figure 8, are JDs 45, 58-60, 65-70, 79, 98, 109, 127 and 139. The one apparent ETC that was not accompanied by an offshore BBL flux was on or about April 07, as suggested by Figure 7 with no offshore flux, and in Figure 8 with no or ~ 0 accumulation in the sediment trap. For that event, Table 1 suggests that the time rate of ETC pressure deepening, DP/Dt, was zero, i.e., 0. So this may have been a mislabeled or misidentified ETC (by the National Weather Service) or a very weak ETC. Over the other seven measurement periods, we can see the up/down trend of sediment accumulation rate exactly matches that of BBL transport, and the two peaks happened exactly at the same time, indicating the significance of BBL transport on the sediment accumulation rate.

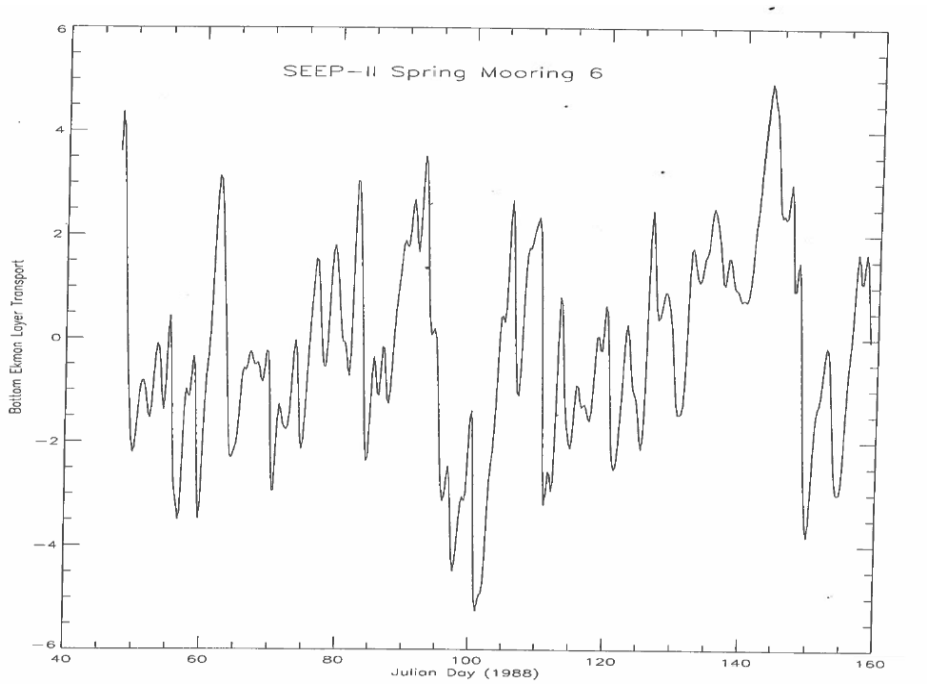

Figure 7. BBL Offshore (+) and Onshore (-) Transport during the spring 1988 period of SEEP II at the base of Mooring 6. Mooring 9 shows a similar plot so is not shown.

Continental shelf and slope bottom regions are often characterized by non-cohesive sediments (Bliven *et al.*, 1977). Near bottom currents with large velocities may cause sediment resuspension on the continental shelf and slope. Previous studies of sediment resuspension have developed threshold criteria, usually an empirical determination of current near ocean bottom,

or of bottom stress that is required to initiate motion of particular sediment grain size (Butman *et al.*, 1979; Komar, 1976; Miller *et al.*, 1977). Once the sediment material is suspended by any of those factors, a mean current can distribute it over a large area. Threshold studies are useful for estimation of sediment motion. The threshold for sediment resuspension events varies from place to place and depends on sediment size. A value of at least 10 cm/s is given by McCave (1972) as the minimum critical value for sediment resuspension for the sediments on the shelf of the MAB. In relatively shallow continental shelf waters, both wave-induced and steady bottom currents contribute to the bottom stress variation and are important mechanisms for suspending sediment particles. Because of the increased bottom stress caused by the oscillatory currents associated with the surface waves in the shallow water on the continental shelf, intense sediment transport and resuspension events are expected during winter storms. Models of the flow field in the bottom boundary layer under combined surface wave and current conditions have been developed by Smith and McLean (1977), Grant and Madsen (1979, 1982) and Grant *et al.* (1984), known as GM79 and GM82. In these models the velocity profile, bottom stress, and the apparent roughness is determined as a function of four inputs: the velocity of the mean current at a reference height above the wave boundary layer, the wave orbital velocity and period, the relative angle between wave and current, the physical bottom roughness. GM79 and GM82 models have been tested in the shallow water fields (generally less than 80 m) under various conditions (Churchill *et al.*, 1994; Lyne *et al.*, 1990; Grant *et al.*, 1984) with good agreement.

Sediment concentrations over the continental shelf during atmospheric storms were estimated by Moody, Butman, and Bothner (1987) and the results are within 50% of the GM model predications. During winter storms, the bottom stress in a water depth of 80 m, was calculated by Lyne *et al.* (1990) using GM models and determined that it exceeded the stress computed from the more conventional quadratic drag law by a factor of 1.4 to 1.6 on average and was a factor of 3 or more during storm peaks. That study concluded that parameterizations of bottom stress that do not incorporate wave effects will grossly underestimate stress and sediment resuspension and transport in the region of continental shelf with water depth less than 100 m. Likewise, Churchill *et al.* (1994) estimated the threshold using the bottom stress computed using GM models and suggested that for the MAB there are at least two thresholds for fine-grained particles, one for those at the sediment surface and another for those incorporated with grained material beneath the sediment surface, and the thresholds are between 0.8 dy cm^{-2} and 2.2 dy cm^{-2}, respectively. Although surface waves interact with bottom currents on the MAB continental shelf, their contribution to the deep-water current may be small. The surface wave field decays with the depth from the free surface and is a mean function of mean depth of the water, the wave velocity near bottom on the continental slope at sites 6 and 9 (400 m) is relatively an unimportant factor. This can be seen very clearly from the surface wave dispersion relation in equation 6.

$$c = \frac{\omega}{k} = \sqrt{\frac{g}{k}} \tanh(kh) \tag{7}$$

where k is the surface wave number, g = 9.8 m/s^2, h is the total water depth, and c is the surface wave phase velocity. Typical surface waves have a period of order 10 s. Using (7) we can get that the surface wave with period of 10 s has a wavelength of about 150 m. Therefore, we can use the deep-water wave approximation to calculate the maximum current velocity associated with the surface waves. The perturbation pressure field associated with deep water waves is given by Gill (1982) as

$$p' = \rho g \eta_0 \cos(kx - \omega t) \exp(-kz) \tag{8}$$

Using (7), we can derive the horizontal velocity field:

$$u = \int -\frac{1}{\rho}\frac{\partial p'}{\partial x}\,dt = \sqrt{gk}\,\eta\cos(kx - \omega t)\exp(-kz) \quad (9)$$

where η is the surface wave amplitude.

The oscillating horizontal velocities associated with surface waves attenuated with water depth, and the e-folding distance is about 24 m from the surface. So even for a very large 10 m amplitude surface wave, the horizontal current velocity associated with it is found, using equation (9), to be virtually zero at depths deeper than 100 m. So, suspension and reworking of sediments by the surface wave process in deep water is weak to unimportant. At moorings 6 and 9 sites, the water depth is 400 m, so we can neglect the surface wave's contribution to the resuspension events on the continental slope in our study region. But the surface wave field does contribute to sediment resuspension events on the continental shelf, where the water depth is shallower than 100 m, on the SEEP II region, and this part of sediment could be transported via the BBL to the continental slope region.

In Figure 8 the mass flux time series from the sediment traps at sites 6 and 9 are plotted along with the dates of the passages of the respective ETCs and TCs. Table 1 summarizes the storm statistics as well as a qualitative indication of the sediment accumulations which were measured at sites 6 and 9 in the sequentially opening and closing sediment traps at 390 m in 400 m of water on both the North and South lines. In both of the TC cases and in 24 of the 26 ETC cases, accumulations were high at least one of the two sites, a 93% overall correlation. Albeit the highly significant finding is that during the passages of the ETCs, in 22 of the 26 cases both "north" and "south" traps filled up contemporaneously, which suggests "across the array" large scale atmospheric and oceanic events. This is an "88%" hit rate favoring bight sized advective events rather than local resuspension phenomena. The two tropical cyclones, Albert and Chris, appeared to be differentially correlated to accumulation increase. The TCs Albert and Chris affected the sediment traps differentially. Albert's track (Figure 4b) was well to the west of the southern array and given its small radius, it did not affect the southern portion of the MAB in any significant way. However, its winds were felt in the central to northern portion of the MAB, and as it passed, its trailing south-southeastward winds were present. Alternatively, TC Chris had a track (Figure 4b) which was well to the east of the SEEP array, being close to the southern transect but not the northern transect. In general, the sediment accumulation rate remains virtually constant across the array and its value was generally very low over the entire summer period on the north line at mooring 6 with its highest value having been recorded between 02-13 August with a minor bump up between 8/24 and 9/02. On the south line there was a major increase between 8/24 and 9/02. So, qualitatively Table 1 and Figures 5, 6 and 7 suggest a correlation between the passages of ETCs, and TCs as well, with periods of high sediment accumulations. Conversely, the figures and table point to a relationship between periods of low sediment accumulations with the lack of occurrence of ETCs or TCs.

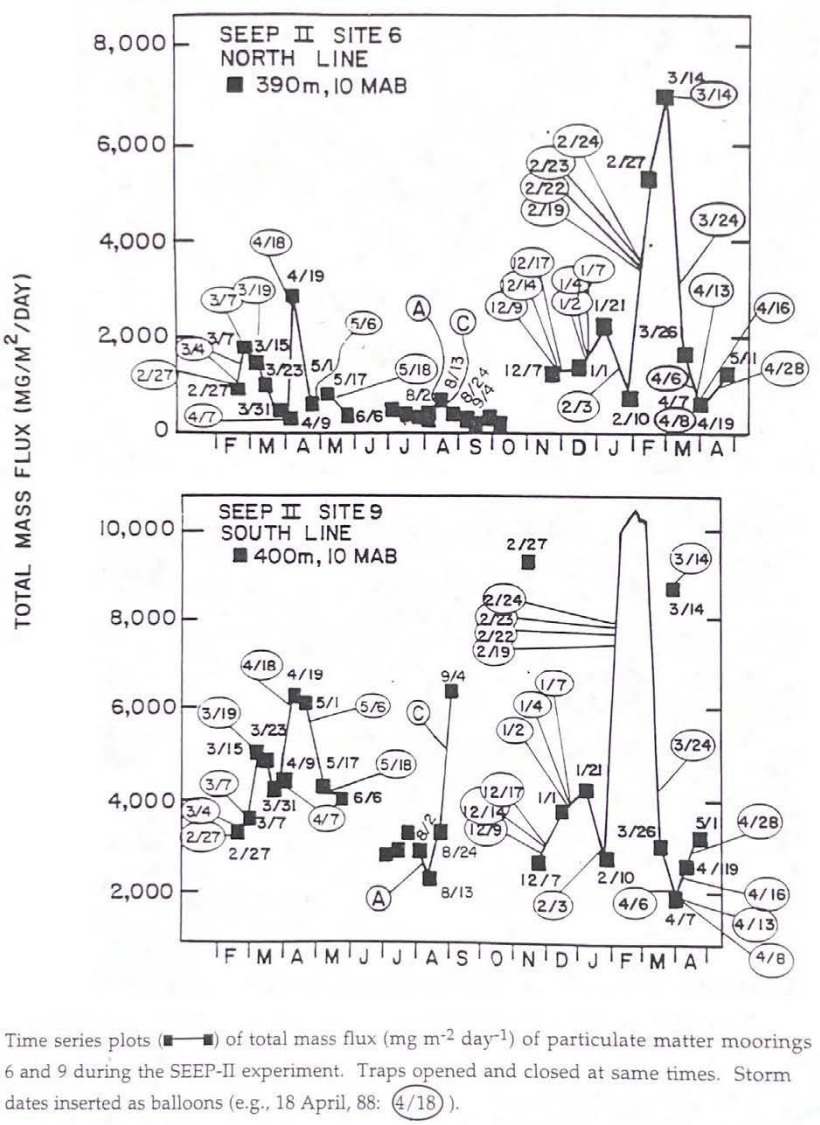

Time series plots (■—■) of total mass flux (mg m^{-2} day^{-1}) of particulate matter moorings 6 and 9 during the SEEP-II experiment. Traps opened and closed at same times. Storm dates inserted as balloons (e.g., 18 April, 88: (4/18)).

Figure 8. Total Sediment Mass Accumulations as a function of Time in the Bottom Sediment Traps at Moorings 6 and 9 during SEEP II. See text for details. However, the plots show that during the passages of 24 of the 26 ETCs and 2 of the 3 TCs sediment accumulations increased rapidly in the Sediment Traps, while periods of Non-Cyclone passages, and were also periods during which there were only modest sediment depositions. These atmospheric cyclone passages are documented in Table 1 and the Total SEEP II sediment accumulations are plotted in Figure 3.

SUMMARY AND DISCUSSION

Our analysis of the extratropical cyclone events during the SEEP-II experiment period showed that total sediment mass flux was highly related to the passages of Extratropical Cyclones. During 24 of 26 ETC passages, the sediment accumulation rate measured on the upper slope of the MAB was found to increase greatly. This finding explains the results by Biscaye and Anderson (1994) and confirms the hypothesis of this paper that extreme short-lived atmospheric storms lasting for several days at a time are responsible for the measured rates of sediment accumulations in the MAB. Thus, the notion that a slow flow to the south with an even slower offshore flux was not supported by the results of this study. During the passages of ETCs, a southwestward alongshore current, in concert with the bottom, was found

to induce offshore bottom Ekman transport. During the passages of ETC and TC events, favorable winds and currents generated large down-shelf alongshore or parabathic, barotropic geostrophic interior currents, and thus via bottom Ekman veering induce large bottom offshore transport. Time averaged currents and BBL transport analysis showed that the sediment accumulation rate was highly related to the alongshore interior current over the entire study area, suggesting large scale phenomena over the entire shelf and upper slope of the MAB.

The RMS of bottom velocities and bottom stress calculated at moorings 6 and 9 represented the bottom current perturbation, and the velocity and stress exceeded the critical value necessary to induce sediment resuspension on several occasions. Although the overall averaged RMS velocity and bottom stress are not large near the bottom at moorings 6 and 9, the RMS current velocity was comparable to the critical value during two periods, and thus were large enough to cause local sediment resuspension. The bottom stress calculated using quadratic law theory showed similar trends as the bottom current RMS velocity plots at both mooring 6 and 9. The sediment particle size distribution over the shelf and slope of MAB are not known in detail and no general resuspension critical current values were set. The two periods when both BBL transport and RMS velocity/bottom stress reached their peaks, the sediment accumulation rate also reached its peak, which more than doubled its average value.

Strong alongshore down-shelf and offshore current components associated with ETC and TC events were found to be the main mechanism for sediment accumulation events over the outer shelf of the MAB. However, during the largest two accumulation events in April 1988 and February 1989, bottom RMS velocities and bottom stresses were large enough to generate local resuspension and thus could have included significant peaks over these two time periods. As relates to the structural integrity of the Shelf-Slope Front (the SSF)), the BBL induced via frictional processes would be sufficiently robust to erode the base of the SSF allowing for the creation of a channel greater than 10 m in thickness through which shelf sediments can flow offshore. Given the steeply sloped bottom, horizontal eddy mixing becomes important and helps to thicken the frictional BBL and increase the offshore transport. The results of this study showed that in order to be able to fully understand the response of the water column and material flux to intense atmospheric forcing it is not sufficient to know that a storm occurred. One must know the track, size and intensity, and duration of the storm to be able to prognosticate the system response. That said, the concept of a continual low frequency flux of sediments fails in comparison to those bottom boundary layer offshore fluxes due to highly energetic cyclone storm passages. The conclusion, Atmospheric Cyclones passing through the MAB cause massive offshore sediment fluxes in a thick bottom boundary layer in the MAB.

ACKNOWLEDGMENTS

The US Department of Energy provided support for this study via a DOE grant to L.J. Pietrafesa. CCU is acknowledged for providing the support to Gayes, Bao and Pietrafesa to process the data sets, produce the plots and write the manuscript. Karl and Arencibia-Perez edited the text. Dr. George Saunders of DOE is acknowledged for having been the visionary and agency driving force behind the SEEP II experiment. Dr. J. Dungan Smith (deceased) is acknowledged for his encouragement of L.J. Pietrafesa and W. Grant (deceased) in their studies of physical processes and in their pursuits of answers to the challenge of continual low frequency material fluxes versus high frequency short period bursts of sediment transport on U.S. continental margins.

REFERENCES

Anderson, R. F., Bopp, R. F., Buesseler, K. O., & Biscaye, P. E. (1988). Mixing of particles and organic constituents in sediments from the continental shelf and slope off Cape Cod: SEEP—I results. *Continental Shelf Research*, *8*(5-7), 925-946.

Biscaye, P. E., & Anderson, R. F. (1994). Fluxes of particulate matter on the slope of the southern Middle Atlantic Bight: SEEP-II. *Deep Sea Research Part II: Topical Studies in Oceanography*, *41*(2-3), 459-509.

Biscaye, P. E., Anderson, R. F., & Deck, B. L. (1988). Fluxes of particles and constituents to the eastern United States continental slope and rise: SEEP—I. *Continental Shelf Research*, *8*(5-7), 855-904.

Biscaye, P. E., Flagg, C. N., & Falkowski, P. G. (1994). The shelf edge exchange processes experiment, SEEP-II: an introduction to hypotheses, results and conclusions. *Deep Sea Research Part II: Topical Studies in Oceanography*, *41*(2-3), 231-252.

Bliven, L., Huang, N. E. & Janowitz, G. S. (1977). *An experimental investigation of some combined flow sediment transport phenomena*. UNC-SG-77-04, Report No. 77-3.

Brink, K. H. (1982). A comparison of long coastal trapped wave theory with observations off Peru. *Journal of Physical Oceanography*, *12*(8), 897-913. https://doi.org/10.1175/1520-0485(1982)012<0897:ACOLCT>2.0.CO;2

Butman, B., Beardsley, R. C., Magnell, B., Frye, D., Vermersch, J. A., Schlitz, R., ... & Noble, M. A. (1982). Recent observations of the mean circulation on Georges Bank. *Journal of Physical Oceanography*, *12*(6), 569-591.

Butman, B., Noble, M., & Folger, D. W. (1979). Long-term observations of bottom current and bottom sediment movement on the mid-Atlantic continental shelf. *Journal of Geophysical Research: Oceans*, *84*(C3), 1187-1205.

Churchill, J. H., Wirick, C. D., Flagg, C. N., & Pietrafesa, L. J. (1994). Sediment resuspension over the continental shelf east of the Delmarva Peninsula. *Deep Sea Research Part II: Topical Studies in Oceanography*, *41*(2-3), 341-363.

Cione, J. J. (1996). *The impact of Gulf Stream-induced diabatic forcing on coastal mid-Atlantic surface cyclogenesis* (Ph.D. Thesis). North Carolina State University, Raleigh.

Cione, J. J., Raman, S., & Pietrafesa, L. J. (1993). The effect of Gulf Stream-induced baroclinicity on US East Coast winter cyclones. *Monthly Weather Review*, *121*(2), 421-430.

Gill, A. (1982). *Atmosphere-ocean dynamics* (Vol. 30). Academic press. https://scholar.google.com/scholar?q=gill+1982+atmosphere+ocean+dynamics+pdf&hl=es&as_sdt=0&as_vis=1&oi=scholart

Grant, W. D., & Madsen, O. S. (1979). Combined wave and current interaction with a rough bottom. *Journal of Geophysical Research: Oceans*, *84*(C4), 1797-1808. https://doi.org/10.1029/JC084iC04p01797

Grant, W. D., & Madsen, O. S. (1982). Movable bed roughness in unsteady oscillatory flow. *Journal of Geophysical Research: Oceans*, *87*(C1), 469-481. https://doi.org/10.1029/JC087iC01p00469

Grant, W. D., Williams III, A. J., & Glenn, S. M. (1984). Bottom stress estimates and their prediction on the northern California continental shelf during CODE-1: The importance of wave-current interaction. *Journal of Physical Oceanography*, *14*(3), 506-527. https://doi.org/10.1175/1520-0485(1984)014<0506:BSEATP>2.0.CO;2

Houghton, R. W., Flagg, C. N., & Pietrafesa, L. J. (1994). Shelf-slope water frontal structure, motion and eddy heat flux in the southern Middle Atlantic Bight. *Deep Sea Research Part II: Topical Studies in Oceanography*, *41*(2-3), 273-306. https://doi.org/10.1016/0967-0645(94)90024-8

Janowitz, G. S. & Pietrafesa, L. J. (1996). Sub-tidal frequency fluctuations in coastal sea level in the Middle and South Atlantic Bights. *Journal of Coastal Research*, *12*(1), 79-89.

Komar, P.D. (1976). The transport of cohesion-less sediments on continental shelves. In D. J. Stanley & D. J. P. Swift (Eds.), *Marine Sediment Transport and Environmental Management* (pp. 107-125). John Wiley, New York.

Luyten, J. R. (1977). Scales of motion in the deep Gulf Stream and across the continent rise. *Journal of Marine Research*, *35*, 49-74.

Lyne, V. D., Butman, B., & Grant, W. D. (1990). Sediment movement along the US east coast continental shelf—I. Estimates of bottom stress using the Grant-Madsen model and near-bottom wave and current measurements. *Continental Shelf Research*, *10*(5), 397-428. https://doi.org/10.1016/0278-4343(90)90048-Q.

McCave, I. N. (1972). Transport and escape of fine-grained sediment from shelf areas. In D.J.P. Swift, D.B. Duane, & O.H. Pilkey (Eds.), *Shelf Sediment Transport: Process and Pattern*. Dowden, Hutchinson & Ross, Stroudsberg.

Miller, M. C., McCave, I. N., & Komar, P. (1977). Threshold of sediment motion under unidirectional currents. *Sedimentology*, *24*(4), 507-527.

Moody, J. A., Butman, B., & Bothner, M. H. (1987). Near-bottom suspended matter concentration on the continental shelf during storms: estimates based on in situ observations of light transmission and a particle size dependent transmissometer calibration. *Continental Shelf Research*, *7*(6), 609-628.

Pedlosky, J. (1979). *Geophysical Fluid Dynamics*. Springer-Verlag.

Pietrafesa, L. J., Brooks, D. A., Amato, R. R. & Atkinson, L. P. (1976). *Onslow Bay Physical/Dynamical Experiments*. UNC Sea Grant Publication, 1-185. https://repository.library.noaa.gov/view/noaa/42243/noaa_42243_DS1.pdf

Roebber, P. J. (1984). Statistical analysis and updated climatology of explosive cyclones. *Monthly Weather Review*, *112*(8), 1577-1589. https://doi.org/10.1175/1520-0493(1984)112<1577:SAAUCO>2.0.CO;2

Sanders, F., & Gyakum, J. R. (1980). Synoptic-dynamic climatology of the "bomb". *Monthly Weather Review*, *108*(10), 1589-1606. https://doi.org/10.1175/1520-0493(1980)108<1589:SDCOT>2.0.CO;2

Shaw, P. T., & Csanady, G. T. (1983). Self-advection of density perturbations on a sloping continental shelf. *Journal of Physical Oceanography*, *13*(5), 769-782. https://doi.org/10.1175/1520-0485(1983)013<0769:SAODPO>2.0.CO;2

Smith, J. D. (1977). Modelling of Sediment Transport on Continental shelves. In E.D. Goldberg (Ed.), *The Sea* (Vol. 6). John Wiley, New York. https://www.osti.gov/servlets/purl/7156268

Smith, J. D., & McLean, S. R. (1977). Spatially averaged flow over a wavy surface. *Journal of Geophysical research*, *82*(12), 1735-1746.

Smith, P. C., & Petrie, B. D. (1982). Low-frequency circulation at the edge of the Scotian Shelf. *Journal of Physical Oceanography*, *12*(1), 28-46.

Verity, P. G., Bauer, J. E., Flagg, C. N., DeMaster, D. J., & Repeta, D. J. (2002). The Ocean Margins Program: An interdisciplinary study of carbon sources, transformations, and sinks in a temperate continental margin system. *Deep Sea Research Part II: Topical Studies in Oceanography*, *49*(20), 4273-4295. https://doi.org/10.1016/S0967-0645(02)00120-0

Walsh, J. J., Biscaye, P. E., & Csanady, G. T. (1988). The 1983–1984 shelf edge exchange processes (SEEP)—I experiment: hypotheses and highlights. *Continental Shelf Research*, *8*(5-7), 435-456. https://doi.org/10.1016/0278-4343(88)90063-5